01000011 01101000 01100001 01110000
01110100 01100101 01110010 00100000
00110010 00101110 00110110 00001010

Chapter 2.7

An anatomical study of the ECRL and ECRB: Feasibility of developing a preoperative test for evaluating the strength of the individual wrist extensors.

Kerver, A.L.A., Carati, L., Eilers, P.H.C., Langezaal, A.C., Kleinrensink, G.J., Walbeehm, E.T.

ABSTRACT

Background: Tendon transfers are essential for reconstruction of hand function in tetraplegic patients. To transfer the extensor carpi radialis longus (ECRL), the extensor carpi radialis brevis (ECRB) has to be sufficiently strong. However, there is currently no reliable clinical test to individually analyse both muscles. In order to develop a reliable preoperative clinical test, the anatomy of the muscle (innervation) areas of ECRB, ECRL and brachio-radialis (BR) was examined.

Methods: In 20 arms, the ECRB, ECRL and BR were dissected and localised. Subsequently, muscle-innervation points were mapped and categorised. A novel method, computer-assisted surgical anatomy mapping (CASAM), was used to visualise muscle areas and innervation points in a computed arm with average dimensions.

Results: For both ECRL and ECRB a 100% area could be identified, a specific area in the computed average arm in which the muscle was present for all 20 arms. For the ECRL, this area was situated at 16% of the distance between the lateral epicondyle and the deltoid muscle insertion. The ECRB 100% area was 5 times bigger than that of the ECRL and was located at 40% of the distance between the lateral epicondyle and the radial styloid process. The ECRL and BR showed one to three innervation points, the ECRB one to four. In 47% of the cases, there was a combined nerve branch innervating both the ECRL and the ECRB.

Conclusions: It is feasible to develop a preoperative test; the 100% areas can be used for needle electromyography (EMG) or local anaesthetic muscle injections.

INTRODUCTION

Damage to the cervical spinal cord represents 60% of all spinal cord injuries.[1] Tetraplegic patients become dependent on external help for daily activities and both productivity and quality of life are lowered significantly.[2,3] The loss of upper limb function can be partially restored with tendon transfers, especially in C4–C6 lesions.[2-4] In these patients, an extensor carpi radialis brevis (ECRB) with motor strength M4 allows for an extensor carpi radialis longus (ECRL) tendon transfer to regain active finger flexion for cylinder grip or to restore thumb opposition.[4,5] However, if the ECRL is transferred without a sufficiently strong remaining ECRB the transferred ECRL will overcome the weaker ECRB and force the wrist in flexion on gripping, decreasing the strength of the grip.

The International Classification for Surgery of the Hand in Tetraplegia (ICSHT) was developed to identify the number of muscles below the elbow with an M4 motor grade or more. In complete spinal cord lesions, it is possible to conclude that if the pronator teres muscle is M4, the ECRB should be M4 also. However, if the pronator teres muscle is not strong enough it is difficult to clinically predict the individual strength of ECRB as both ECRL and ECRB have the same function in wrist movement.

In incomplete spinal cord lesions, muscle function does not follow a specific pattern and it usually is difficult to assign an ICSHT level to these patients.[6,7] Therefore, it is particularly important to evaluate the to-be-transferred ECRL. Moreover, in these patients functional outcome after tendon transfer is unpredictable; if the ECRL muscle shows evidence of abnormal regeneration during needle electromyography (EMG), it will probably perform poorly if transferred.[6]

Previously, several tests have been proposed to individually evaluate the function of ECRL and ECRB but these tests were either invasive (Moberg and House[8, 9]) or unreliable (Mohammed and Rothwell[4]).

In order to develop such a reliable test, knowledge of the anatomical relationship of the individual muscles in the forearm and their motor-innervation points is the first step. Although described in mainstream anatomy textbooks,[5,10] the present study provides a new way of visualising data of multiple specimens in one combined image using computer assisted surgical anatomy mapping (CASAM).[11-13]

METHODS

General

In this study 20 arms (11 left and 9 right) from 20 embalmed human bodies, flushed with Anubifix,[14] were used. The borders of the ECRB, ECRL and brachio-radialis (BR) were dissected and marked with pins.

'Bony' landmarks were assessed and used as a reference for measurements. In order to define the dimensions of each arm, 'non-bony' or 'shape-defining' landmarks were calculated from bony landmarks and positioned on the outer contour of each arm (Figure 1). Reproducibility of the landmarks was tested and the landmarks were assessed by two authors.
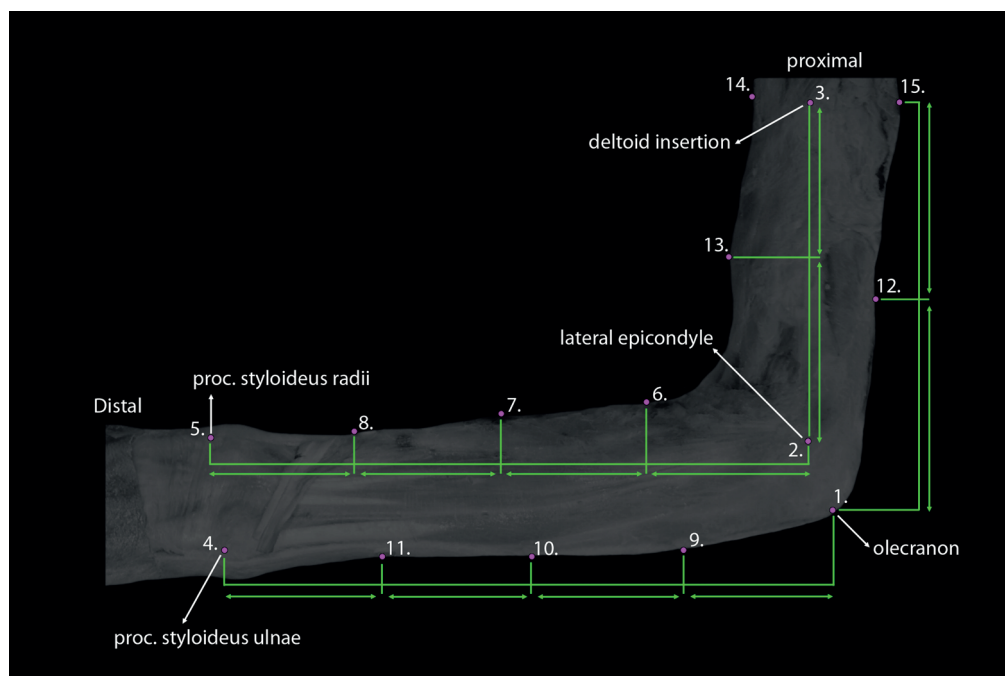

Figure 1. Landmarks.
Bony landmarks: the most lateral and proximal part of the olecranon (1), the lateral epicondyle (2), the deltoid muscle insertion on the humerus (3), the ulnar styloid process (4) and the radial styloid process (5). Non-bony or shape defining landmarks: at one fourth (6), halfway (7) and three fourth (8) between landmark 2 and 5. At one fourth (9), halfway (10) and three fourth (11) between landmark 1 and 4. Halfway between landmark 1 and 3 (12) and halfway between landmark 2 and 3 (13). Two landmarks were placed on the most medial (14) and the most lateral (15) edge of the upper arm at the level of landmark 3.

Each arm was photographed using a Nikon D60 with a Sigma 50 mm 1:2.6 DG macro lens. The arm was positioned in 90° flexion. A 100-mm reference ruler was placed next to the arm. Raw images were loaded into Photoshop CS-4.[15] Digital measurements were taken using the 'ruler tool' and calibrated with the ruler.

General assessments: The distance between the lateral epicondyle and the radial styloid process was measured to define the length of the forearm.

Computer-Assisted Surgical Anatomy Mapping (CASAM)

CASAM[11] is a new method to compare and evaluate the anatomy of multiple specimens. First, using the landmarks (Figure 1) the shape of each photographed specimen is defined and an average shape is calculated from all 20 specimens. With MagicMorph,[16] each specimen in each original picture is reshaped/warped to match the calculated average shape. MagicMorph uses a thin plate spline transformation as a warping algorithm. Then, as all reshaped specimens have the same average shape, the anatomy can be compared. In Photoshop CS-4, the reshaped photographs can be loaded into stack and the relevant anatomy can be highlighted. Finally, renditions can be made to simultaneously visualise the anatomy of multiple specimen in one picture (e.g., the location of the ECRL of 20 specimens shown in one computed averagely shaped arm).

In all 20 warped specimens, the ECRB, ECRL and BR were highlighted and data on the muscle locations of all 20 specimens were compiled into one image. To visualise the variance in anatomy three zones were computed:

1) 100% area. In this area of the average arm the muscle is present in all 20 specimens. Thus, in each individual specimen, the muscle can be found within the 100% area.
2) 50% area. In this area the muscle is present in 10–19 of the 20 specimens. Thus, in a specific specimen, there is a 50–95% chance that the muscle can be found in the 50% area.
3) General area of distribution. In this area the muscle was present in one to nine of the 20 specimens.

Description on the course of the ECRB, ECRL and BR

CASAM is a novel method of anatomy mapping and therefore the data needed to be evaluated in a more conventional way. Measurements were taken every 10 mm from a virtual line between the lateral epicondyle and the radial styloid process (Figures 2 and 3).

Statistical Package for Social Sciences (SPSS) 17 was used to perform basic statistical analysis of the data and to produce graphs:

1) Tables were standardised on the x-axis for the length of the forearm and on the y-axis for the length of the arm (deltoid muscle insertion and the lateral epicondyle).
2) The x- and y-axes were divided into a grid of small squares. To squares inside the region where a muscle is located, the number 1 is added for each specimen. The result is a grid of counts, each showing how many of the individual muscles cover the corresponding squares.
3) A smoothing procedure was applied to the histogram to reduce the influence of sampling variation.17

The statistical procedure is described for one way of standardisation. The principle is the same for the width of the muscles, except no standardisation on the y-axis was applied.

Innervation

The innervating nerves of the ECRB, ECRL and BR were dissected. The radial nerve was localised and the muscular branches, the superficial radial branch and the posterior interosseous nerves were dissected. The (extramuscular-) motor-innervation points of each muscle were marked with pins, digitally mapped and projected on the computed, average-sized arm using CASAM. Finally, the branches innervating the muscles were categorised.

RESULTS

General measurements

Collective intrinsic measurements and locations computed with CASAM were expressed as a percentage of either the length of the (upper-) arm or the forearm. The arm is defined as a scale ranging from the lateral epicondyle (0%) towards the deltoid muscle insertion (100%). The forearm is defined as a scale ranging from the lateral epicondyle (0%) towards the radial styloid process (100%).

The mean distance between the lateral epicondyle and the radial styloid process is 24.92 cm (range 21.5–27.5 cm).

Measurements on the course of the ECRB, ECRL and BR

The anatomical localisation of the ECRB, ECRL and BR is highly variable (Figures 2 and 4).

Brachio-radialis

In the CASAM assessment, there is no area in which all BR muscles of all 20 specimens are present. The 50% area and the general area of distribution show much overlap distally with the ECRL. The main direction of variation is in the width of the muscle (Figure 4). Further, in the SPSS assessment the BR shows the most variation in anatomical localisation (Figure 2.2). In a maximum of 80% of the arms, the muscle is present at the same location. This area is located near
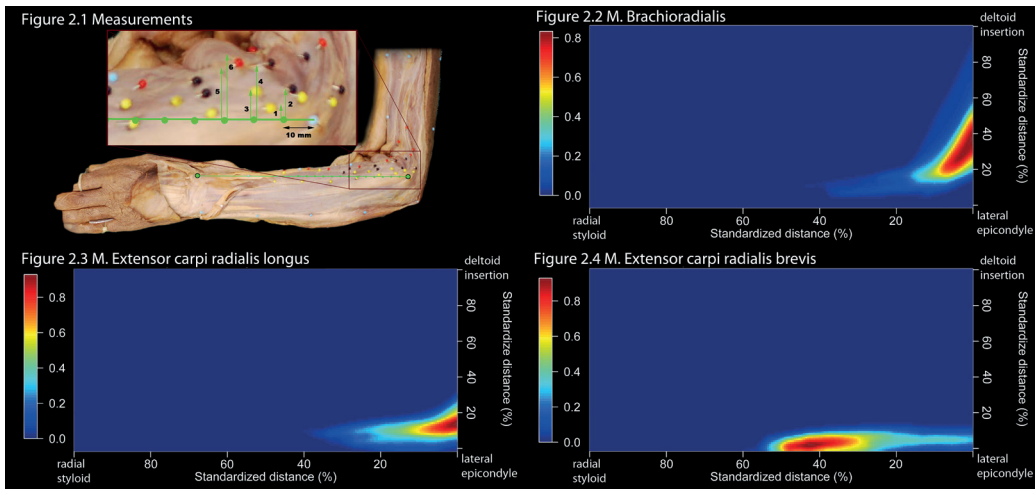

Figure 1. The location of the BR, ECRL and ECRB.
2.1 Measurements taken. Landmarks and axes used. Red pins: borders of the BR. Red pins: borders of the ECRL. Yellow pins: borders of the ECRB. 1: to the nearest part of the ECRB. 2: to the furthest part of the ECRB. 3: to the nearest part of the ECRL. 4: to the furthest part of the ECRL. 5: to the nearest part of the BR. 6: to the furthest part of the BR. 2.2 the location of the BR in all 20 arms. Dark red depicts the location in which the BR was present in 80% of the arms. Dark blue depicts the location in which the muscle was not present. 2.3 the location of the ECRL. Dark red depicts the location in which the ECRL was present in 100% of the arms. Dark blue depicts the location in which the muscle was not present. 2.4 the location of the ECRB. Dark red depicts the location in which the ECRB was present in 100% of the arms. Dark blue depicts the location in which the muscle was not present. Figures 2.2, 2.3 and 2.4 were standardised on the x-axis for the length of the lower arm and on the y-axis for the length of the upper arm. X-axis: the distance between the lateral epicondyle (0) and the radial styloid process (100). Y-axis: the distance between the lateral epicondyle (0) and the m. deltoid insertion on the humerus (100).

the origin of the BR at a level of 45% of the length of the arm. In all 20 arms, the width of the BR is 2.0–8.2 cm. The BR is widest near its origin (Figure 3.2).

Extensor carpi radialis longus

In the CASAM assessment the ECRL only has a small area in which the muscle is always present, the 100% area (Figure 4). This area is situated at a level of 16% of the arm, close to the origin of the muscle (Figure 5). The 50% area is larger but proximally shows much overlap with the general area of distribution of the BR. Distally the 50% area shows overlap with the general area of distribution of the ECRB (Figure 4). In the SPSS assessment the ECRL is also relatively variable (Figure 2.3). An area can be identified in which the muscle is present in all 20 arms. This 100% area is located near the origin of the ECRL at a level of 17% of the arm. The main direction of variation is in the length of the ECRL. In all 20 arms the muscle is 1.1–4.0 cm wide. The ECRL is widest near its origin (Figure 3.3).
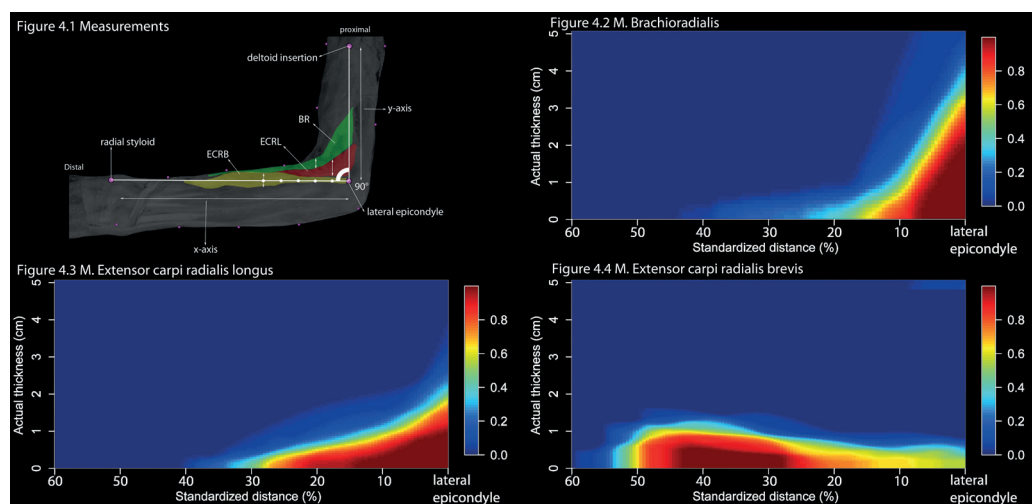

Figure 3. The width of the BR, ECRL and ECRB.
3.1, measurements taken, landmarks used for both x-axis and y-axis. 3.2, the width of the BR. 3.3 the width of the ECRL. 3.4, the width of the ECRB. X-axis: the distance between the lateral epicondyle (0) and the radial styloid process (100). Y-axis: the actual thickness of the muscles. Dark red depicts 80% (in 3.2) or 100% (in 3.3 and 3.4) of all muscles. Dark blue depicts 0% of all muscles.
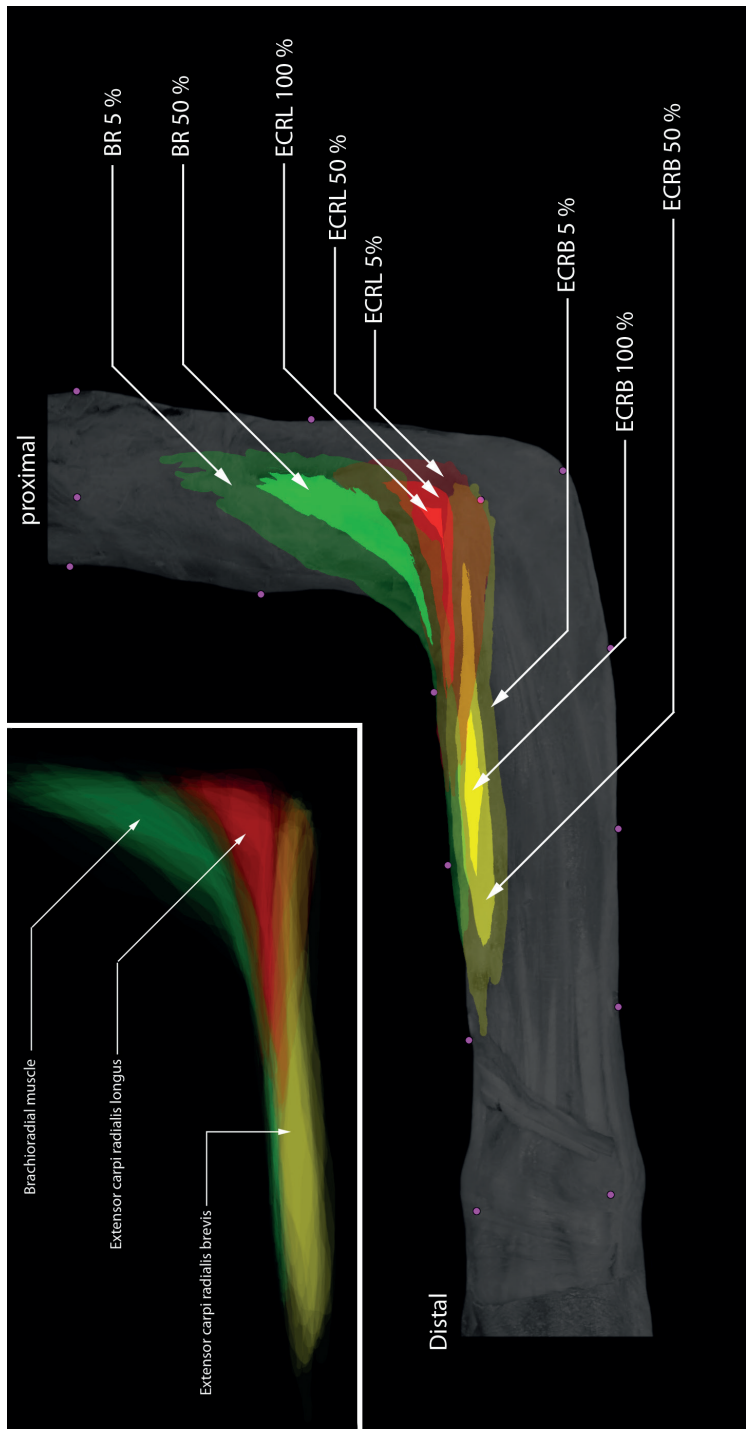
Figure 4. Spreading of the BR, ECRL and ECRB.
Original overlay of all muscles (top left) and subsequent renditions of the 5%, 50% and 100% area of spreading of the BR, ECRL and ECRB (N = 20). Purple dots: landmarks used for warping.
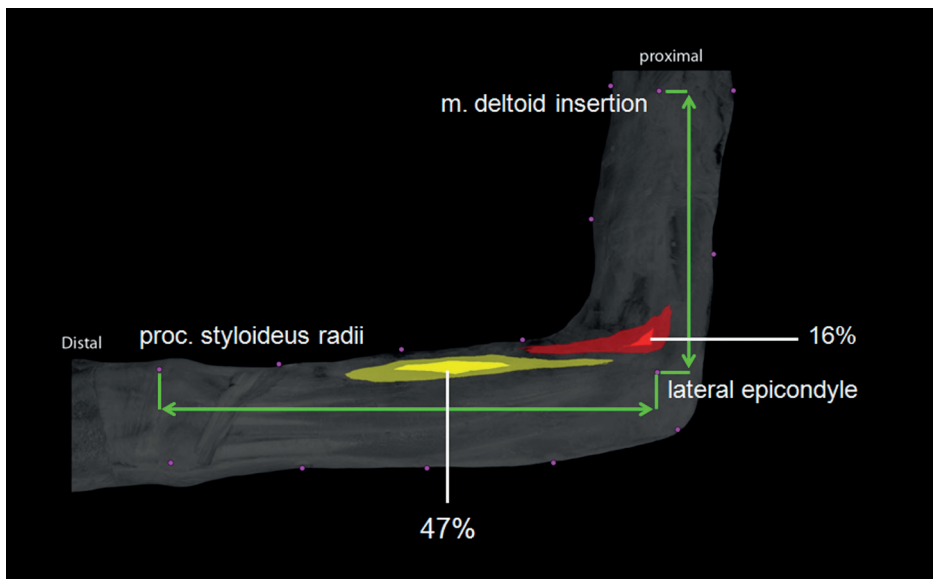
Figure 5.The 100% and 50% area of spreading of the ECRL and ECRB.
Purple dots: landmarks. Red: extensor carpi radialis longus. Yellow: extensor carpi radialis brevis.
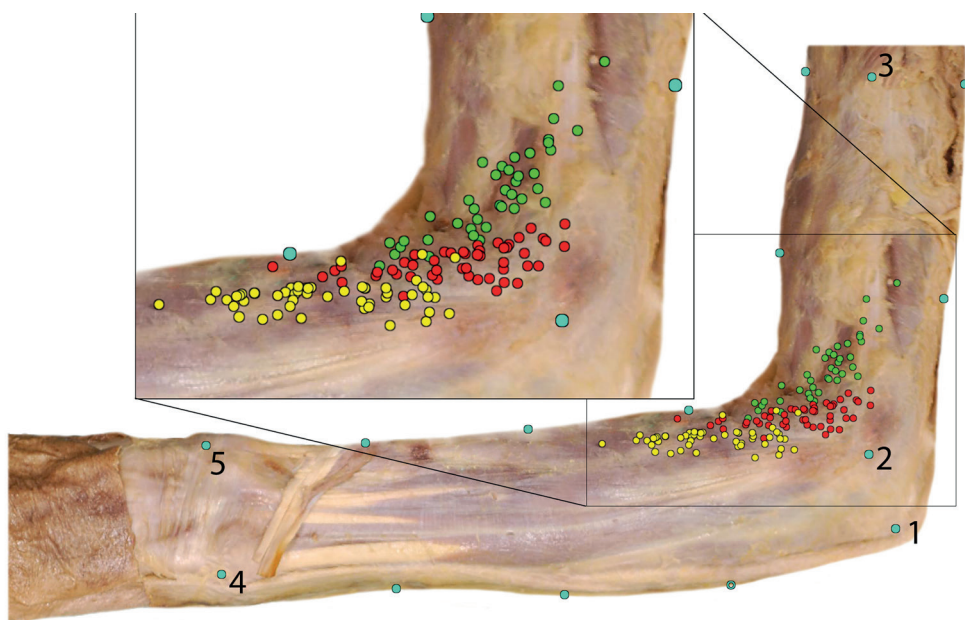

Figure 6. Spreading of the innervations of the BR, ECRL and ECRB.
Blue dots: landmarks. Green dots: motor innervations of the BR (N = 40). Red dots: motor innervations of the ECRL (N = 49). Yellow dots: motor innervations of the ECRB (N = 49).

Extensor carpi radialis brevis

In the CASAM assessment, the general variation in the localisation of the ECRB origin is relatively low. The 20 dissected muscles show a large area in which the muscle is always present, the 100% area (Figure 4). This area is situated at a level of 47% of the forearm. The 100% area of the ECRB is 4.8 times bigger than the 100% area of the ECRL. The area in which the muscle is present in 50% is not much larger than the 100% area, but proximally it shows an overlap with the general area of distribution of the ECRL (Figure 4). With SPSS, the ECRB also is the least variable and an area can be identified in which the muscle is located in all 20 specimens (Figure 2.4). This area is found at a level of 45% of the forearm and is substantially larger than the 100% area of the ECRL (Figure 2). The main direction of variation is in the length of the muscle. The widest part of the muscle is located at a level of 45% of the forearm. The ECRB shows the least variation in width, with a range of 0.6–1.6 cm at the widest part of the muscle (Figure 3.4).

Innervation

The BR on average had 2.0 (range 1–3) extra-muscular motor-innervation points, which were consistently located close to the 50% area of the BR. The ECRL had 2.5 (range 2–3) motor-innervation points, which were located distal to the 100% area of the ECRL. The ECRB had 2.45 (range 2–4) motor-innervation points, which were located proximal to the 100% area of the ECRB.

The highest density of motor-innervation points for ECRL and ECRB together is located at a level of 16% of the forearm. The average level of motor-innervation points for the ECRB is located at a level of 24% of the forearm and for the ECRL at a level of 10% of the forearm (Figure 6). The motor-innervation points were categorised in two main variations (Figure 7):

1) Variations with a combined branch which innervates both the ECRL and the ECRB (N = 9). The combined branch originates from the deep branch of the radial nerve (RN), or the posterior interosseous nerve (PIN) or the superficial radial nerve (SRN).
2) Variations without a combined branch (N = 10).

The BR has one or two direct innervations originating from the RN and in addition to a possible combined branch, the ECRL has one or two direct innervations from the RN.

If a combined branch originates from the RN or SRN, the ECRB is additionally innervated by one or two branches from the SRN. If the combined branch originates from the PIN, the ECRB is additionally innervated by one, two or three branches from the PIN. If no combined branch is present, the ECRB is in innervated by both the SRN and PIN (N = 8) or only by the SRN (N = 2).

One arm could not be categorised as the origin of one of the branches to the ECRL could not be located.
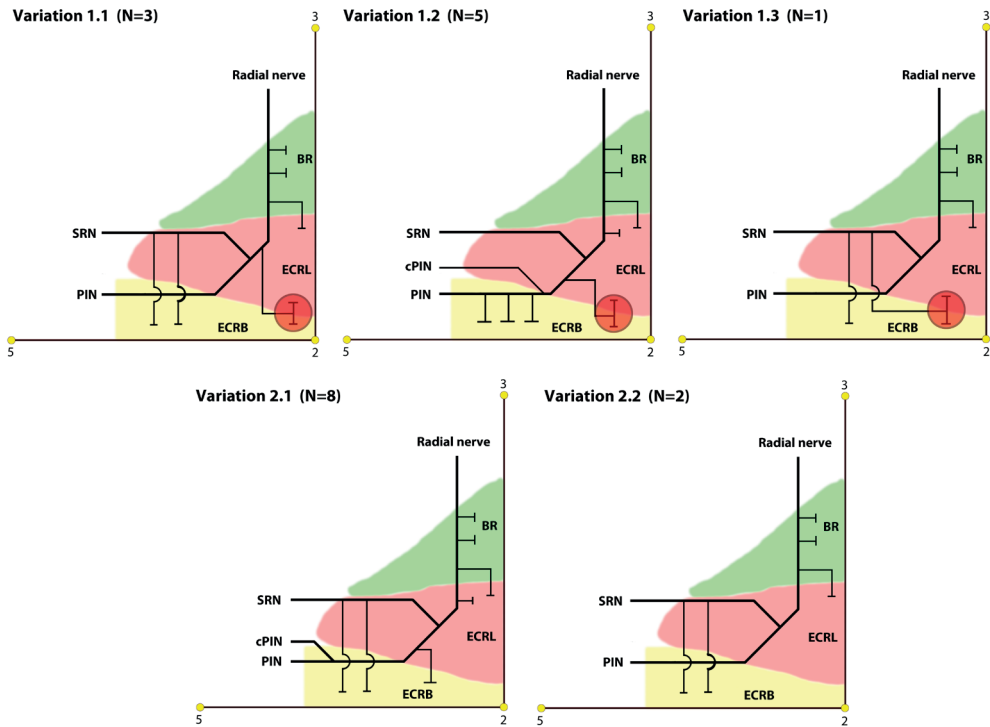

Figure 7. Categorisation of innervations of the BR, ECRL and ECRB.
Yellow dots: landmarks used, 2 = lateral epicondyle, 3 = deltoid muscle insertion, 5 = radial styloid process. SRN: superficial radial nerve, PIN: posterior interosseous nerve. cPIN: concomitant posterior interosseous nerve. Variation 1 (N = 9): combined branch: innverating both the ECRL and ECRB. It originates either from the deep branch of the radial nerve (1.1), the posterior interosseous nerve (1.2) or the superficial radial nerve (1.3). ECRB: one or two direct innervations from the superior radial nerve (1.1, 1.3) or one to three innervations from the posterior interosseous nerve (1.2). Variation 2 (N = 10): No combined branch to the ECRL and ECRB is present. ECRB: one or two direct innervations from the posterior interosseous nerve and two or three direct innervations from the superficial radial nerve (2.1) or only two or three direct innervations from the superficial radial nerve (2.2).

DISCUSSION

For a successful ECRL tendon transfer, both the ECRL and the ECRB need to be sufficiently strong (M4–M5). At present, no reliable clinical test is available to independently test the function of the ECRB and ECRL. Knowledge of the anatomical relationship of the individual muscles is a first step in the development of a reliable clinical test.

Location of muscles

As described in the literature,[10, 18-20] considerable variation is found in the anatomy of the radial wrist extensors. The ECRB, ECRL and BR of all 20 specimens show much overlap. Therefore, non-invasive identification of muscle bellies is difficult and complicates the development of a clinical test. Nevertheless, two distinct 100% areas are identified for the ECRB and ECRL. In such an area, the respective muscle is found at that location in all 20 specimens (100%) and has no overlap with any other muscles. For the ECRB, this 100% area is situated at a level of 47% of the forearm (Figure 5). This corresponds to the needle-insertion location for individual EMG of the ECRB proposed by Riek et al. (47.58% of forearm length).[21]

Similarly, for the ECRL the 100% area is located near its origin at a level of 16% of the arm (Figure 5). This area does not correspond to needle-insertion locations found in the literature.[21, 22]

Further, both ECRB and ECRL are widest near their respective 100% areas. Clinically, these findings allow for non-invasive identification and use in the clinical testing of both muscles.

The 100% area of the ECRB is 4.8 times bigger when compared to the 100% area of the ECRL. In theory, it would be easier to identify the ECRB and use it for a clinical test. However, a drawback of this study is that healthy, non-tetraplegic arms were used. This poses two problems for extrapolation to clinical practice. Afflicted muscles of tetraplegic patients are likely to be atrophic upon clinical presentation and their anatomy might consequently differ from the anatomy described. As the 100% area of the ECRL is much closer to its origin than the 100% area of the ECRB, there will be less variation in the 100% area of the ECRL between healthy and atrophic muscles.

The small width of the ECRB (0.6–1.6 cm) and ECRL (1.1–4.0 cm) does not allow for surface EMG, especially since surface EMG is prone to have crosstalk from more distant sources.[23, 24] Further, the amount of overlap between the ECRB and ECRL could cause considerable crosstalk and therefore lead to inaccurate

test results. Calder et al.[25] however showed that surface EMG results of the radial wrist extensors are more reliable than needle EMG though they did not distinguish between ECRB and ECRL.

Motor-innervation points

The number of (extramuscular) motor-innervation points for ECRB and ECRL varies widely in the literature. We found that the ECRL had two or three motor-innervation points, in contrast to one or two[26] or on average 3.8 motor innvervations.[27] The ECRB had two to four motor-innervation points; this contrasts with findings of Nayak et al. (one motor innervation)[5] and is more in accordance with El-Din Safwat et al. (two to five motor innervations)[28] and Abrams et al. (on average 3.4 motor innervations).[27]

The wide variability of the origin of ECRB branches has been well described. In accordance with current literature,[5, 26, 27] we found that the ECRB can be innervated by the RN, PIN and/or SRN.

However, we also found a singular combined branch innervating both ECRB and ECRL, present in 45% of the specimens. This combined branch might affect test results when the ECRL is injected with a local anaesthetic; due to diffusion of the local anaesthetic the entire combined branch, and therefore also the (proximal) branch innervating the ECRB, might be affected. Succeeding wrist function tests might therefore give lower results in 45% of patients. In local anaesthetic nerve block of the ECRL branch,[29] the combined branch might be missed resulting in incomplete paralysis of the ECRL, or if the combined branch is effectively paralysed part of the ECRB will be paralysed also.

The highest density of motor-innervation points for ECRL and ECRB together is located at a level of 16% of the forearm, which correlates to the site most used for needle EMG of the radial wrist extensors: 4 cm distal to the lateral epicondyle = 16% of the average forearm length.[22]

The location of motor innervations of ECRB and ECRL showed overlap. This overlap might provoke crosstalk in surface EMG measurements. Further in local anaesthetic ECRL nerve blocks,[29] some branches to the ECRB might be affect ed.

Motor innervations of the ECRB were located proximal to the 100% area, whilst those of the ECRL were located distally to its respective 100% area. Although still controversial, functional electrical stimulation has been used to enhance recovery in central nerve lesions. Popovic et al. stated that the efficiency of intramuscular electrical stimulation is reduced when electrodes are placed further away from the motor-innervation points of the muscle.[30] As most motor-innervation points of the ECRB and ECRL are not located near their respective

100% areas, the 100% areas should not be used for electrode placement. Instead, the electrodes should be placed at the level of 24% and 10% of the length of the forearm for the ECRB and the ECRL, respectively.

CONCLUSION

Local anaesthetic muscle injection: analogous to the preoperative testing with Marcaïne of brachialis and BR muscles in biceps to triceps transfers. [31, 32] Both ECRB and ECRL have a 100% area that can be used for local anaesthetic muscle injection. As the tendon of the ECRL is usually transferred, the individual function of the ECRB determines the postoperation wrist extension. After injecting the ECRL, the individual function of the ECRB can be tested. However, the combined branch should be taken into account as the local anaesthetic might diffuse to the ECRB branch and affect succeeding test results.

Local anaesthetic nerve block of the ECRL branch: as proposed by Genet et al. [29] Both the combined branch present in 45% of the specimens and the overlap between motor-innervation points of ECRB and ECRL will influence the outcome of succeeding function tests of the ECRB.

Surface EMG: analogous to the muscle activity assessment of the vastus intermedius.[33, 34] Anatomically, it is not feasible to individually assess motor function of ECRB and ECRL using surface EMG.

Needle EMG: Most literature on needle EMG indicates that it is not possible to differentiate between ECRB and ECRL.[25, 35] However, the distinct 100% areas for the ECRB (47% of the length of the forearm) and ECRL (16% of the length of the (upper-) arm) found in this study suggest it is. These areas allow for accurate needle placement in the intended muscle and thus the individual function of ECRB and ECRL can be examined directly.

ACKNOWLEDGEMENTS

REFERENCES

1) Lamb, D.W., Chan, K.M. Surgical reconstruction of the upper limb in traumatic tetraplegia. A review of 41 patients (1983) Journal of Bone and Joint Surgery - Series B, 65 (3), pp. 291-298.

2) Cizmar, I., Zalesak, B., Pilny, J., Drac, P., Fialova, J. Possible restorations of the upper extremity motion in tetraplegic patients - 5-year clinical experience. (2006) Biomedical papers of the Medical Faculty of the University Palacký, Olomouc, Czechoslovakia, 150 (2), pp. 313-319.

3) Freehafer, A.A. Gaining independence in tetraplegia: Cleveland technique (1998) Clinical Orthopaedics and Related Research, (355), pp. 282-289.

4) Mohammed, K.D., Rothwell, A.G., Sinclair, S.W., Willems, S.M., Bean, A.R. Upper-limb surgery for tetraplegia (1992) Journal of Bone and Joint Surgery - Series B, 74 (6), pp. 873-879.

5) Nayak, S.R., Krishnamurthy, A., Prabhu, L.V., Rai, R., Ranade, A.V., Madhyastha, S. Anatomical variation of radial wrist extensor muscles: A study in cadavers (2008) Clinics, 63 (1), pp. 85-90.

6) Hentz, V.R., Leclercq, C. The Management of the Upper Limb in Incomplete Lesions of the Cervical Spinal Cord (2008) Hand Clinics, 24 (2), pp. 175-184.

7) Ditunno Jr., J.F., Cohen, M.E., Hauck, W.W., Jackson, A.B., Sipski, M.L. Recovery of upper-extremity strength in complete and incomplete tetraplegia: A multicenter study (2000) Archives of Physical Medicine and Rehabilitation, 81 (4), pp. 389-393.

8) Moberg, E. Surgical rehabilitation of the upper limb in tetraplegia (1990) Paraplegia, 28 (5), pp. 330-334.

9) Moberg, E. Surgical treatment for absent single hand grip and elbow extension in quadriplegia: principles and preliminary experience (1975) Journal of Bone and Joint Surgery - Series A, 57 (2), pp. 196-206.

10) William, P.L., Warwich, R., Dyson, M., Bannister, L.H. (1989) The Muscles of the Forearm. Gray's Anatomy, p. 622.

11) Kerver, A.L.A., Van Der Ham, A.C., Theeuwes, H.P., Eilers, P.H.C., Poublon, A.R., Kerver, A.J.H., Kleinrensink, G.-J. The surgical anatomy of the small saphenous vein and adjacent nerves in relation to endovenous thermal ablation (2012) Journal of Vascular Surgery, 56 (1), pp. 181-188.

12) Van Der Graaf, T., Verhagen, P.C.M.S., Kerver, A.L.A., Kleinrensink, G.-J. Surgical anatomy of the 10th and 11th intercostal, and subcostal nerves: Prevention of damage during Lumbotomy (2011) Journal of Urology, 186 (2), pp. 579-583.

13) Ten Berge, M.G., Yo, T.I., Kerver, A., De Smet, A.A.E.A., Kleinrensink, G.-J. Perforating veins: An anatomical approach to arteriovenous fistula performance in the forearm (2011) European Journal of Vascular and Endovascular Surgery, 42 (1), pp. 103-106.

14) http://anubifix.com/English.html

15) Adobe Corp. Adobe Photoshop CS-4
http://www.adobe.com/nl/products/photoshop/photoshop/

16) EffectMatrix Software Studio. Cited 1 time. Magic Morph 1.95
http://www.effectmatrix.com/morphing/

17) Eilers, P.H.C., Goeman, J.J. Enhancing scatterplots with smoothed densities (2004) Bioinformatics, 20 (5), pp. 623-628.

18) Caetano, F.M., Albertoni, M.W., Caetano, B.E., Perez, M.R. Anatomical study of insertions of the extensor carpi radialis longus and brevis (2004) Int J Morphol, 22, pp. 245-251.

19) Albright, J.A., Linburg, R.M. Common variations of the radial wrist extensors (1978) Journal of Hand Surgery, 3 (2), pp. 134-138.

20) MacAlister, A. Additional observations on muscular anomalies in human anatomy with a catalogue of the principal muscular variations hitherto published (third series) (1871) Trans Ir Acad Dublin, 25, pp. 101-102.

21) Riek, S., Carson, R.G., Wright, A. A new technique for the selective recording of extensor carpi radialis longus and brevis EMG (2000) Journal of Electromyography and Kinesiology, 10 (4), pp. 249-253.

22) Misra, U.K., Kalita, J. (1999) Clinical Neurophysiology.

23) Gerdle, B., Karlsson, S., Day, S., Djupsjöbacka, M. (1999) Acquisition, Processing and Analysis of the Surface Electromyogram. Modern Techniques in Neuroscience. Chapter 26, pp. 705-755.

24) Farina, D., Merletti, R., Indino, B., Graven-Nielsen, T. Surface EMG Crosstalk Evaluated from Experimental Recordings and Simulated Signals: Reflections on Crosstalk Interpretation, Quantification and Reduction (2004) Methods of Information in Medicine, 43 (1), pp. 30-35.

25) Perotto, A.O. (1994) Anatomical Guide for the Electromyographer: The Limbs and Trunk.

26) Ravichandiran, M., Ravichandiran, N., Ravichandiran, K., McKee, N.H., Richardson, D., Oliver, M., Agur, A.M. Neuromuscular partitioning in the extensor carpi radialis longus and brevis based on intramuscular nerve distribution patterns: A three-dimensional modeling study (2012) Clinical Anatomy, 25 (3), pp. 366-372.

27) Abrams, R.A., Ziets, R.J., Lieber, R.L., Botte, M.J. Anatomy of the radial nerve motor branches in the forearm (1997) Journal of Hand Surgery, 22 (2), pp. 232-237.

28) Safwat, M.D.E.-D., Abdel-Meguid, E.M. Distribution of terminal nerve entry points to the flexor and extensor groups of forearm muscles: An anatomical study (2007) Folia Morphologica, 66 (2), pp. 83-93.

29) Genet, F., Autret, K., Schnitzler, A., Lautridou, C., Bernuz, B., Denormandie, P., Allieu, Y., Parratte, B. Motor branch of extensor carpi radialis longus: Anatomic localization (2012) Archives of Physical Medicine and Rehabilitation, 93 (12), pp. 2309-2312.

30) Popovic, D., Gordon, T., Rafuse, V.F., Prochazka, A. Properties of implanted electrodes for functional electrical stimulation (1991) Annals of Biomedical Engineering, 19 (3), pp. 303-316.

31) Kozin, S.H., D'Addesi, L., Chafetz, R.S., Ashworth, S., Mulcahey, M.J. Biceps-to-Triceps Transfer for Elbow Extension in Persons With Tetraplegia (2010) Journal of Hand Surgery, 35 (6), pp. 968-975.

2

32) Endress, R.D., Hentz, V.R. Biceps-to-triceps transfer technique (2011) Journal of Hand Surgery, 36 (4), pp. 716-721.

33) Watanabe, K., Akima, H. Validity of surface electromyography for vastus intermedius muscle assessed by needle electromyography (2011) Journal of Neuroscience Methods, 198 (2), pp. 332-335.

34) Watanabe, K., Akima, H. Cross-talk from adjacent muscle has a negligible effect on surface electromyographic activity of vastus intermedius muscle during isometric contraction (2009) Journal of Electromyography and Kinesiology, 19 (4), pp. e280-e289.

35) Riek, S., Bawa, P. Recruitment of motor units in human forearm extensors (1992) Journal of Neurophysiology, 68 (1), pp. 100-108.

2